TÜBİTAK

Turk J Elec Eng & Comp Sci, Vol.18, No.3, 2010, © TÜBİTAK
doi:10.3906/elk-0912-3

Implementation of method for operating multiple high frequency surface wave radars on a common carrier frequency

Ryan RIDDOLLS
Defence Research and Development Canada—Ottawa
3701 Carling Avenue, Ottawa ON K1A 0Z4, CANADA
e-mail: ryan.riddolls@drdc-rddc.gc.ca

Abstract

The increasing use of High Frequency Surface Wave Radar (HFSWR) for the surveillance of coastal regions is faced with the problem of limited channel availability in the electromagnetic spectrum. Thus, there is a need for multiple radars to share a common frequency channel. Proof-of-concept work is presented here for a method to operate multiple radar systems on a common carrier frequency. A review is provided of an existing concept where a common waveform is modulated by tones varying by a few hertz across the different radars. The signals from the different radars are separated by either pulse-domain filtering or Doppler processing. An experiment has been performed that demonstrates the feasibility of the method. Limitations of the method are considered in terms of the linearity of the propagation channel.

Key Words: *High frequency, surface wave radar, common frequency, doppler processing, ionosphere*

1. Introduction

In this paper, we examine proof-of-concept work on a method to operate multiple High Frequency Surface Wave Radar (HFSWR) systems on a common carrier frequency. Operation on a common carrier frequency is advantageous for a network of HFSWR systems due to the limitation of available frequency channels in the electromagnetic spectrum. The use of coding methods to share carrier frequencies is a well-established technique. An existing method has been selected for investigation due to its ease of implementation in practical radar systems. This method is described in Section 2. An experiment is described in Section 3 that tests the method using the ionosphere as a target. The intent of the experiment is to simulate transmissions from two radars on the ground, both producing ionospheric clutter echoes, and show that the echoes from the individual radars can be resolved within the signal processing of each radar. This method is demonstrated for the case of simple pulsed radar transmissions. However, similar results can be expected for more complicated phase code or continuous waveform radars.

Although this experiment can show proof of principle, due to limitations of time and cost it cannot explore all possible values of radar parameters of power, antenna gain, and integration time, which could be encountered during HFSWR operations. In particular, at higher effective radiated powers, the propagation channel for HFSWR clutter signals in the ionosphere becomes significantly nonlinear, and nearby signal frequencies from different radars can become coupled. Some consideration of this effect follows from work that has been carried out in so-called ionospheric heating experiments, where high-power HF waves are deliberately injected into the ionosphere to stimulate nonlinear plasma behaviour. It is shown in Section 4 that the signal power levels associated with typical HFSWR systems do not put the propagation channel into a sufficiently nonlinear state to prevent the radars from operating effectively under the proposed frequency sharing scheme.

2. Common frequency waveforms

Let us consider a single radar employing a waveform $s(t)$ of duration T. For radar applications, we desire that $s(t)$ have good autocorrelation properties, that is the function

$$\chi(\tau) = \int s(t)s^*(t+\tau)\,dt, \tag{1}$$

should be well-confined to an interval in τ on the order of the reciprocal of the bandwidth of $s(t)$. For N radars to share a channel, we might desire that the p^{th} and q^{th} radar waveforms, denoted $s_p(t)$ and $s_q(t)$, where $0 \le p, q \le N-1$, have the cross-correlation property that

$$\chi_{pq}(\tau) = \int s_p(t)s_q^*(t+\tau)\,dt \approx \delta_{pq}\chi(\tau), \tag{2}$$

where δ_{pq} is the Kronecker delta function, and $\chi(\tau)$ is again a well-confined function of τ. In other words, we desire good autocorrelation properties and zero cross-correlation. Waveforms with these properties can be easily constructed when the duration of the waveform is NT [1-3]. Thus, if one is willing to accept a factor-of-N reduction in Doppler bandwidth, and thus a similar reduction in maximum unambiguous target velocity, one can easily share a frequency channel among N radars.

A class of waveforms was suggested in [4,5] that do not obey the zero cross-correlation property of (2) but can still be separated after matched filtering. The concept is to take a radar waveform $s(t)$ of duration T, concatenate N of these waveforms together, and modulate the sequence of waveforms with a continuous complex sinusoid. The p^{th} radar would output an effective waveform of length NT given by

$$s_p(t) = \sum_{n=0}^{N-1} s(t-nT)e^{j2\pi pt/NT}, \tag{3}$$

where $0 \le p \le N-1$. To illustrate how such signals could be separated, we consider a superposition of radar waveforms denoted by $S(t)$:

$$S(t) = \sum_{p=0}^{N-1} A_p s_p(t), \tag{4}$$

where A_p is some complex amplitude. Let us compute the correlation $\chi_m(\tau)$ of $S(t)$ and the shifted waveform $s(t - mT)$, where $0 \leq m \leq N - 1$:

$$\chi_m(\tau) = \int_{mT}^{(m+1)T} \sum_{n=0}^{N-1} \sum_{p=0}^{N-1} A_p s(t - nT) s^*(t - mT + \tau) e^{j2\pi pt/NT} dt. \tag{5}$$

Since $s(t)$ is zero outside of the interval $(0, T)$, we can shift the integration interval by mT as follows:

$$\chi_m(\tau) = \int_0^T s(t) s^*(t + \tau) \sum_{p=0}^{N-1} A_p e^{j2\pi p(t+mT)/NT} dt \tag{6}$$

$$= \sum_{p=0}^{N-1} A_p e^{j2\pi pm/N} \int_0^T s(t) s^*(t + \tau) e^{j2\pi pt/NT} dt. \tag{7}$$

The integral is equal to the ambiguity function for $s(t)$ evaluated at $(\tau, p/NT)$, which we will denote as $\chi(\tau, p/NT)$:

$$\chi_m(\tau) = \sum_{p=0}^{N-1} A_p \chi(\tau, p/NT) e^{j2\pi pm/N}. \tag{8}$$

Thus, we have a sum of the ambiguity functions modulated by tones in the pulse domain. One can now construct linear combinations of the matched filter outputs $\chi_m(\tau)$ that will separate the signals. Let us consider the linear combinations

$$D_q = \sum_{m=0}^{N-1} \chi_m(\tau) e^{-j2\pi qm/N}. \tag{9}$$

The intent is that when $q = p$, the linear combination D_q will contain only the signal corresponding to radar p. The summation D_q is equivalent to Doppler processing, although in the usual Doppler processing operation, one would Fourier transform across a number of waveform repetitions much larger than N in order to resolve finer velocity behaviour of the targets. If we insert χ_m from (8) into the previous equation, then we have

$$D_q = \sum_{p=0}^{N-1} N \delta_{pq} A_p \chi(\tau, p/NT) = N A_q \chi(\tau, q/NT). \tag{10}$$

Since the various radar signals are encoded with different sinusoidal modulations, as an alternative to the summation D_q one can apply filtering methods in the pulse domain to remove the other radar signals. Due to start-up transients in any filtering operation, the state of the filter would have to be preserved across the boundaries of the coherent integration interval of the radar.

3. Experimental results

Experiments using the method described in Section 2 were carried out during August 2004 in Ashton, Ontario, Canada. A photograph of the Ashton site is shown in Figure 1.

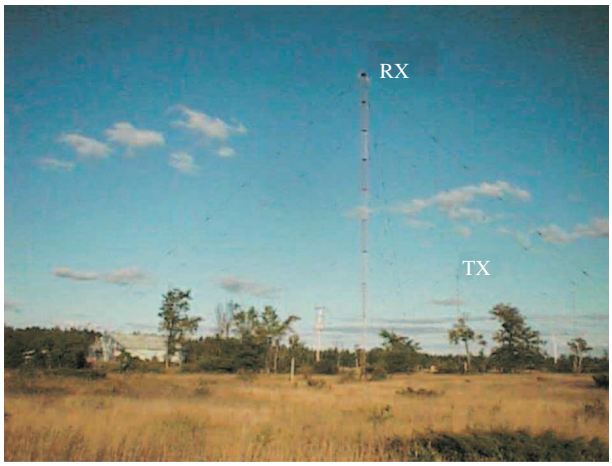

Figure 1. Ashton site.

Visible in the foreground of the photograph is a tower on which is mounted a large loop antenna that is used to receive the radar echoes. A similar loop antenna is mounted on the transmit tower, which is located approximately 150 meters from the receive tower, and is visible in the background of the photograph. Both loops are oriented approximately in the magnetic east-west direction, and consist of an isosceles triangle approximately 10 meters tall and 45 meters wide. A short, broad antenna shape was chosen in order to avoid the need to climb the towers during antenna installation. At 10 meters height, the apex of the loop is close enough to the ground that it can be affixed to the tower by means of a long pole and hook. The 45-meter base is chosen so that the antenna is resonant at a frequency of 3.24 MHz. The impedance is approximately 200 ohms resistance and 0 ohms reactance at resonance. The antenna is matched to 50-ohm coaxial cable using a high-power 4:1 balun. The antennas are fed from a building on the site (visible in the left side of the photograph in Figure 1) via buried coaxial cable runs.

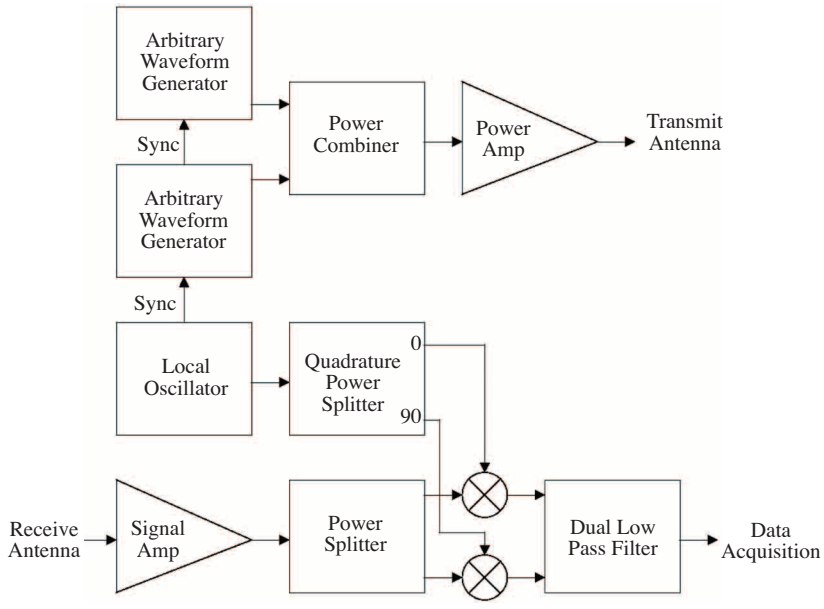

Figure 2. Common frequency experiment apparatus.

A block diagram of the apparatus for the experiment is given in Figure 2. A local oscillator at 3.2425 MHz provides the reference frequency for the transmit and receive subsystems. On the transmit side, two arbitrary waveform generators output radar pulses at frequencies of 3.242500 MHz and 3.242505 MHz, respectively. The pulse shape is a Blackman window with a duration of 250 μs and a repetition rate of 200 Hz. The pulse times of the arbitrary generators are aligned such that both pulses go through a 1-kW power amplifier at the same time. This leads to the formation of intermodulation products. However, the radiated power at the intermodulation product frequencies is sufficiently low during this experiment that the products are not visible in the data.

On the receive side, the local oscillator feeds a standard quadrature demodulator. The data acquisition is laptop-based, with two receive channels each running at 100 kilosamples/second. Limitations to the data acquisition software resulted in a maximum sampling period of two seconds, which is equivalent to 400 transmit pulses.

Attempts to obtain ionospheric echoes using the above apparatus were made during several nights in August 2004. Echoes were achieved on 31 August 2004. An example of a data set acquired at approximately 2300 local time is shown in Figure 3. The data set shows the production of ionospheric echoes at frequencies of 3.242500 MHz and 3.242505 MHz. The echoes extend to about 600 km in range. The average background noise level is about 47 dB in this figure, and the peak signal strength is about 77 dB. SNRs higher than 30 dB could be achieved by arranging an experiment with higher transmit power, higher gain antennas, and longer integration times.

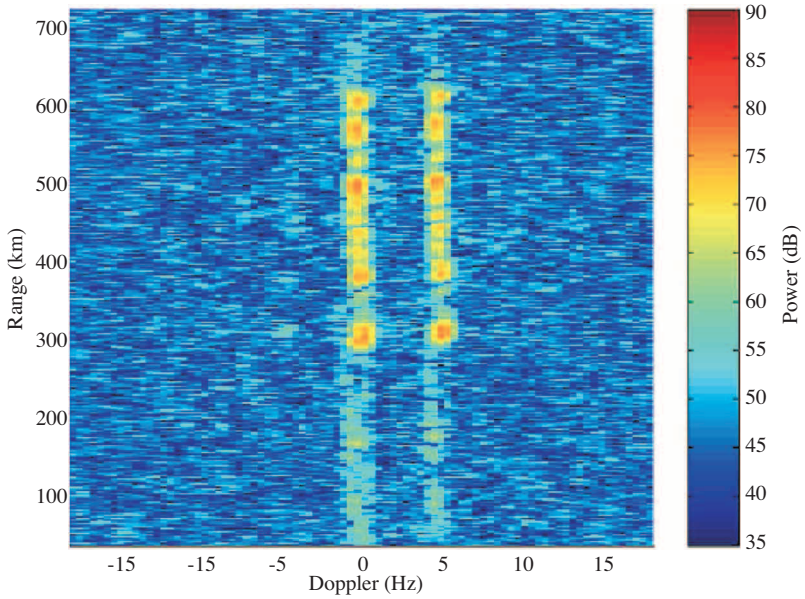

Figure 3. Common frequency experiment results.

The echoes displayed in Figure 3 can be viewed as a confirmation of the method described in Section 2. In the radar waveforms described by (3) we have set $s(t)$ equal to a Blackman window of 250-μs length, with $N = 40$ and $T = 5$ ms. The Doppler bandwidth of a 5-ms waveform is equal to 200 Hz. The 200-Hz bandwidth is shared among 40 radars, resulting in effective Doppler channels of 5-Hz width. In this experiment, two of these effective Doppler channels are populated with radar signals. A total of 400 radar pulses are Doppler-processed, which provides 10 Doppler resolution cells for each Doppler channel. The echoes shown in Figure 3 occupy

approximately 3 Doppler resolution cells due to windowing of the data set prior to Doppler processing.

4. Limitations of method

The frequency sharing method and experiment described above is a transmission of a common radar waveform modulated by N tones, each spaced by a frequency $1/NT$. This corresponds to a spacing in Doppler of typically a few hertz. While the experiments did not reveal nonlinear effects, it should be expected that for large amplitude signals, nonlinearities in the propagation medium can cause HFSWR ionospheric clutter echoes associated with one radar to spread into Doppler frequencies associated with the other radars by the formation of intermodulation products.

We estimate the intermodulation product levels by examining the physics of the plasma near the signal reflection layer. A model of the ionosphere consists of a dielectric medium with permittivity

$$\epsilon = \epsilon_0 \left(1 - \frac{e^2 n_e}{\epsilon_0 m_e \omega^2}\right) \equiv \epsilon_0 \left(1 - \frac{\omega_p^2}{\omega^2}\right), \tag{11}$$

where e is the charge on an electron, n_e is the plasma density, ϵ_0 is the permittivity of free space, m_e is the mass of an electron, ω is the incident wave frequency, and ω_p is defined as the plasma frequency. An upgoing HF wave reflects from the ionosphere at the point where the ionospheric plasma density is sufficient that the right side of (11) is zero. We now examine the plasma dynamics near this reflection layer.

4.1. The ponderomotive force

In this section, we describe the physical processes producing the nonlinear effects during wave propagation in the ionospheric medium, following [6]. Near the reflection height we assume the electric and magnetic fields form a standing wave pattern that can be described in the general form

$$\mathbf{E}(\mathbf{r}, t) = \mathbf{E}(\mathbf{r}) \cos \omega t \tag{12}$$

$$\mathbf{B}(\mathbf{r}, t) = -\nabla \times \mathbf{E}(\mathbf{r}) \frac{\sin \omega t}{\omega}. \tag{13}$$

These fields accelerate charged particles in the plasma according to the Lorentz force law, where the force per unit volume is given by

$$\mathbf{F} = nm \frac{d\mathbf{v}}{dt} = nq(\mathbf{E} + \mathbf{v} \times \mathbf{B}). \tag{14}$$

Here, n is the particle density, m is the mass of a particle, $\mathbf{v}$ is the particle velocity, and q is the particle charge. We treat $\mathbf{E}$ as a small perturbation to the equilibrium, which leads to small perturbations in $\mathbf{B}$ and $\mathbf{v}$. Equation (14) is solved by keeping terms that are first order in the perturbation parameter. The first-order solution is then substituted back into the equation, and the equation is solved for all second-order terms. Since the term $\mathbf{v} \times \mathbf{B}$ is second order in perturbation, the first-order Lorentz equation is given by simply

$$\mathbf{F}_1 = nq\mathbf{E}_1 = nq\mathbf{E}(\mathbf{r}) \cos \omega t, \tag{15}$$

where the subscript is the order of the perturbation. The first-order position and velocity of the particles is thus given by

$$\mathbf{r}_1 = -\frac{q\mathbf{E}(\mathbf{r})}{m\omega^2}\cos\omega t \tag{16}$$

$$\mathbf{v}_1 = \frac{q\mathbf{E}(\mathbf{r})}{m\omega}\sin\omega t. \tag{17}$$

The first-order dynamics involve sinusoidal oscillation in the imposed fields. We now consider the second-order terms in the Lorentz force equation:

$$\mathbf{F}_2 = nq(\mathbf{E}_2 + \mathbf{v}_1 \times \mathbf{B}_1). \tag{18}$$

The second-order electric field $\mathbf{E}_2$ arises from the excursion of the charged particles into regions of different field intensity during the sinusoidal first-order motion:

$$\mathbf{E}_2 = (\mathbf{r}_1 \cdot \nabla)\mathbf{E}(\mathbf{r})\cos\omega t. \tag{19}$$

This term can be recognized as second order since it contains the product of two first-order factors. Combining the previous four equations, the second-order force is

$$\mathbf{F}_2 = -\frac{nq^2\cos^2\omega t}{m\omega^2}[\mathbf{E}(\mathbf{r})\cdot\nabla]\mathbf{E}(\mathbf{r}) + \frac{nq^2\sin^2\omega t}{m\omega^2}[\nabla\times\mathbf{E}(\mathbf{r})]\times\mathbf{E}(\mathbf{r}). \tag{20}$$

Using the vector identity

$$(\mathbf{A}\cdot\nabla)\mathbf{A} = \frac{1}{2}\nabla|\mathbf{A}|^2 + (\nabla\times\mathbf{A})\times\mathbf{A}, \tag{21}$$

and time-averaging, we find there is a DC component of $\mathbf{F}_2$:

$$< \mathbf{F}_2 >= \mathbf{F}_p \equiv -\frac{nq^2}{4m\omega^2}\nabla|\mathbf{E}(\mathbf{r})|^2. \tag{22}$$

$\mathbf{F}_p$ is called the ponderomotive force, which serves to expel particles from regions of high electric field strength. In an electron-ion plasma, the total force on the ionized species is dominated by the electron component, since the force varies inversely with m. The ponderomotive force on the plasma is therefore given by (22) with $q = -e$, $n = n_e$, and $m = m_e$.

4.2. Perturbation of reflection height

The ponderomotive force generally produces a plasma cavity that grows until the force is balanced by the plasma pressure gradient:

$$\mathbf{F}_p = \nabla n_e \kappa T, \tag{23}$$

where κT is the electron energy. Assuming homogeneous temperature, we have

$$\nabla n_e = -\frac{e^2 n_e}{4\omega^2 m_e \kappa T}\nabla|\mathbf{E}(\mathbf{r})|^2. \tag{24}$$

If we integrate this equation from above the reflection height, where there is no electric field, to the center of the cavity, we find that the fractional density depletion is given by

$$\frac{\Delta n_e}{n_e} = -\frac{e^2|\mathbf{E}(\mathbf{r})|^2}{4\omega^2 m_e \kappa T}. \tag{25}$$

The consequence of this result is that the plasma density at the reflection height is reduced, meaning that the wave now reflects at a greater height. This altitude increase creates a phase perturbation (α) to the radar signal, which we expect should increase with the power of the signal. Numerical integration of the wave equation in linear ionosphere profiles [7] shows that this phase perturbation is linearly proportional to power flux, with a value of approximately $\alpha = 7\times10^3$ rad $\mathrm{W}^{-1}\,\mathrm{m}^2$. We now calculate the size of the intermodulation products, following [7]. The incident wave field near the reflection height can be written as the sum of two carrier frequencies a few hertz apart:

$$E_i = \frac{E_0}{2}\cos(\omega_1 t) + \frac{E_0}{2}\cos(\omega_2 t) \tag{26}$$

$$= E_0 \cos\left[\frac{(\omega_1-\omega_2)t}{2}\right]\cos\left[\frac{(\omega_1+\omega_2)t}{2}\right]. \tag{27}$$

We can consider the $E_0\cos[(\omega_1-\omega_2)t/2]$ factor to be the instantaneous amplitude of a carrier wave at frequency $(\omega_1+\omega_2)/2$. The reflected wave will have a phase lag ϕ proportional to the incident wave power that is given by

$$\phi = \frac{\alpha E_0^2}{2\eta}\cos^2\left[\frac{(\omega_1-\omega_2)t}{2}\right] \tag{28}$$

$$= \frac{\alpha E_0^2}{4\eta}\left\{1+\cos\left[(\omega_1-\omega_2)t\right]\right\}, \tag{29}$$

where η is the impedance of free space. Ignoring constant phase terms, the reflected wave is

$$E_r = \frac{E_0}{2}\cos\left\{\omega_1 t - \frac{\alpha E_0^2}{4\eta}\cos\left[(\omega_1-\omega_2)t\right]\right\}$$

$$+\frac{E_0}{2}\cos\left\{\omega_2 t - \frac{\alpha E_0^2}{4\eta}\cos\left[(\omega_1-\omega_2)t\right]\right\}. \tag{30}$$

The cosine factors can be expanded so that we can write

$$E_r = \frac{E_0}{2}[\cos(\omega_1 t)+\cos(\omega_2 t)]\cos\left\{\frac{\alpha E_0^2}{4\eta}\cos[(\omega_1-\omega_2)t]\right\}$$

$$+\frac{E_0}{2}[\sin(\omega_1 t)+\sin(\omega_2 t)]\sin\left\{\frac{\alpha E_0^2}{4\eta}\cos[(\omega_1-\omega_2)t]\right\}. \tag{31}$$

We now make use of the identities

$$\cos(z\cos\beta) = J_0(z) - 2J_2(z)\cos(2\beta)+\cdots \tag{32}$$

$$\sin(z\cos\beta) = 2J_1(z)\cos\beta - 2J_3(z)\cos(3\beta) + \cdots, \tag{33}$$

where $J_\nu(z)$ is the ordinary Bessel function of order ν. We find that the reflected field is given by

$$\begin{aligned} E_r = {} & \frac{E_0}{2} J_0\left(\frac{\alpha E_0^2}{4\eta}\right)[\cos(\omega_1 t) + \cos(\omega_2 t)] \\ & + \frac{E_0}{2} J_1\left(\frac{\alpha E_0^2}{4\eta}\right)\{\sin(\omega_1 t) + \sin(\omega_2 t) \\ & + \sin[(2\omega_1 - \omega_2)t] + \sin[(2\omega_2 - \omega_1)t]\} \\ & - \frac{E_0}{2} J_2\left(\frac{\alpha E_0^2}{4\eta}\right)\{\cos[(2\omega_1 - \omega_2)t] + \cos[(2\omega_2 - \omega_1)t] \\ & + \cos[(3\omega_1 - 2\omega_2)t] + \cos[(3\omega_2 - 2\omega_1)t]\} - \cdots. \end{aligned} \tag{34}$$

Since $\alpha E_0^2/(4\eta) \ll 1$, we have $1 \approx J_0 \gg J_1 \gg J_2$, therefore

$$\begin{aligned} E_r \approx {} & \frac{E_0}{2}[\cos(\omega_1 t) + \cos(\omega_2 t)] \\ & + \frac{E_0}{2} J_1\left(\frac{\alpha E_0^2}{4\eta}\right)\{\sin[(2\omega_1 - \omega_2)t] + \sin[(2\omega_2 - \omega_1)t]\} \\ & - \frac{E_0}{2} J_2\left(\frac{\alpha E_0^2}{4\eta}\right)\{\cos[(3\omega_1 - 2\omega_2)t] + \cos[(3\omega_2 - 2\omega_1)t]\} - \cdots. \end{aligned} \tag{35}$$

The power of the kth intermodulation product relative to the carrier is thus

$$\frac{P_i}{P_s} \approx J_k^2\left(\frac{\alpha E_0^2}{4\eta}\right), \tag{36}$$

where P_s is the carrier power and P_i is the intermodulation product power. To estimate this ratio for typical HFSWR systems, we take an average power of 1 kW, and consider two nearby radars with 0 dBi gain in the general direction of the ionosphere (at around 300 km range, but not necessarily directly overhead). The radiation from the two radars will be coherent and thus will quadruple in power for a maximum power flux of about $E_0^2/(2\eta) = 4\times10^{-9}$ W/m^2. Inserting this value into (36) gives a $k = 1$ intermodulation product level of -103 dB, which is sufficiently low for the case of ionospheric clutter that is limited to about 60 dB SNR in typical HFSWR systems [8].

5. Conclusion

This paper has discussed the implementation of a method that allows multiple radars to share a frequency channel. Section 2 reviewed an existing scheme that consists of modulating a common waveform by a set of tones that are spaced at frequency intervals of the waveform repetition rate divided by the number of radars (N) sharing the channel. Section 3 provided experimental demonstration of the $N = 40$ waveforms, where two simulated radars produced signals that are separable by the operation of Doppler processing. Section 4 showed

that signal intermodulation due to ionospheric nonlinearity is negligible up to SNR levels of approximately 100 dB. In conclusion, the proposed method is a good candidate for sharing of frequency channels among N radar systems so long as the radar operator can accept a reduction in maximum observable target velocity by a corresponding factor of N.

References

[1] Y. I. Abramovich, G. J. Frazer. "Bounds on the volume and height distributions for the MIMO radar ambiguity function." *IEEE Signal Processing Letters*, Vol. 15, pp. 505-508, 2008.

[2] D. E. Barrick, P. M. Lilleboe, C. C. Teague. "Multi-station HF FMCW radar frequency sharing with GPS time modulation multiplexing." United States Patent 6856276, 2005.

[3] R. J. Riddolls. "Extended Frank codes and their application to the sharing of radar frequency channels." DRDC Ottawa TM 2004-216, Defence R&D Canada—Ottawa, 2004.

[4] V. F. Mecca, J. L. Krolik, F. C. Robey, D. Ramakrishnan. "Slow-time MIMO spacetime adaptive processing." *MIMO Radar Signal Processing*, New York, Wiley, 2009.

[5] A. M. Ponsford, R. Dizaji, R. R. McKerracher. "System and method for concurrent operation of multiple radar or active sonar systems on a common frequency." United States Patent 7151483, 2006.

[6] F. Chen. *Introduction to Plasma Physics and Controlled Fusion*. New York: Plenum Press, 1984.

[7] Z. H. Huang, J. A. Fejer. "Nonlinear sidebands of two powerful waves at closely spaced frequencies in the ionosphere." *Radio Science*, Vol. 22, pp. 663-670, 1987.

[8] H. C. Chan. "Characterization of ionospheric clutter in HF surface-wave radar." DRDC Ottawa TR 2003-114, Defence R&D Canada—Ottawa, 2003.